Observation of repetitively nanosecond pulse-width transverse patterns in microchip self-*Q*-switched laser

Jun Dong* and Ken-ichi Ueda

Institute for Laser Science, University of Electro-Communications, 1-5-1 Chogugaoka, Chofu, Tokyo 182-8585, Japan

(Received 18 January 2006; published 31 May 2006)

Repetitively nanosecond pulse-width transverse pattern formation in a plane-parallel microchip Cr,Nd: yttrium-aluminum-garnet (YAG) self-*Q*-switched laser was investigated. The complex point-symmetric transverse patterns were observed by varying the pump beam diameter incident on the Cr,Nd:YAG crystal. The gain guiding effect and the thermal effect induced by the pump power in microchip Cr,Nd:YAG laser control the oscillating transverse modes. These transverse pattern formations were due to the variation of the saturated inversion population and the thermal induced index profile along radial and longitudinal direction in the Cr,Nd:YAG crystal induced by the pump power incident on the Cr,Nd:YAG crystal. These were intrinsic properties of such a microchip self-*Q*-switched laser. The longitudinal distribution of the saturated inversion population inside the gain medium plays an important role on the transverse pattern formation. Different sets of the transverse patterns corresponds to the different saturated inversion population distribution inside microchip Cr,Nd:YAG crystal.

PACS number(s): 42.60.Jf, 42.65.Sf, 42.60.Gd, 42.55.Sa

I. INTRODUCTION

The phenomenon of spontaneous transverse pattern formation in optical systems has been an interesting topic in recent years [1]. Transverse pattern formation has been achieved in CO_2 lasers [2,3]. The complex transverse patterns observed in CO_2 lasers could be interpreted as the simultaneous excitation of empty cavity eigenmodes, this implies that the patterns are dominated by boundary effects rather than by the nonlinearity of the gain medium. In addition, CO_2 lasers were usually achieved by using long cavities in which the longitudinal-mode spacing was in the same order of magnitude as the transverse-mode spacing [4]. Recently, transverse pattern formation has been observed in vertical cavity surface emitting semiconductor lasers with large transverse cross section and short cavity length [5,6]. Although vertical cavity surface emitting semiconductor lasers could be easily operated in single-longitudinal-mode oscillation and were used to study transverse pattern formation eliminating the influence of other degrees of freedom, the main difficulty for transverse pattern formation analysis was that the pattern formation was strongly sensitive to the inhomogeneity of the semiconductor wafers. Laser-diode-pumped microchip solid-state lasers have gained much attention for studying the transverse pattern formation recently [7–10]. Because laser-diode pumped microchip laser can be easily operated in single-longitudinal-mode oscillation, the dynamics of the transverse mode oscillation for laser-diode pumped microchip laser can be fully investigated. There are some experimental and theoretical investigations on the transverse mode pattern formation of laser-diode pumped microchip solid-state lasers [11,12]. However, these microchip lasers were usually operated in continuous-wave mode and the transverse patterns were investigated mostly around the threshold. The pattern formation above the threshold was

not investigated. Most of applications of the pattern formation require laser pulses with high peak power, which can be realized by passively *Q*-switched solid-state lasers. Passively *Q*-switched solid-state lasers with high peak power are usually achieved by using high gain medium and Cr^{4+}: yttrium-aluminum-garnet (YAG) crystal as saturable absorber [13]. Recently there are some reports on the laser instabilities of Cr^{4+}:YAG passively *Q*-switched Nd:YAG lasers induced by the transverse mode competition [14,15]; the transverse pattern formations were observed in a passively *Q*-switched Nd:YVO_4 laser with Cr^{4+}:YAG as the saturable absorber, different sets of transverse patterns were observed by varying the cavity length. However, these experimental results strongly depend on the cavity parameters and the spot diameter of the intracavity beam on the saturable absorber, and so on. To fully understand the nonlinear effects of the saturable absorber and gain medium on the transverse pattern formation of the passively *Q*-switched laser, a microchip Cr,Nd:YAG laser will be a very good arena because a Cr,Nd:YAG self-*Q*-switched laser crystal combining gain medium ions, Nd^{3+} and saturable absorber, Cr^{4+} into one. Microchip Cr,Nd:YAG self-*Q*-switched lasers with sub-nanosecond pulse width have been demonstrated [16,17]. Microchip configuration eliminates the influence of the cavity parameters; the transverse pattern formation only depends on the pump beam diameter and the nonlinear effects of the gain medium and saturable absorber. Because of the planar-parallel nature of the cavity, the transverse eigenmodes of microchip lasers are determined not by the mirror curvatures but rather by the gain guiding effect or thermal guiding effect induced by the pump beam [11,12]. However, these theories treated the transverse modes in microchip lasers with one-dimensional models for simplicity [11,12], the effect of longitudinal distribution of the pump power inside the gain medium was not addressed. In fact, the longitudinal distribution of the pump power inside the gain medium has a great effect on the transverse pattern formation; different transverse patterns can be obtained by varying the pump beam diameter

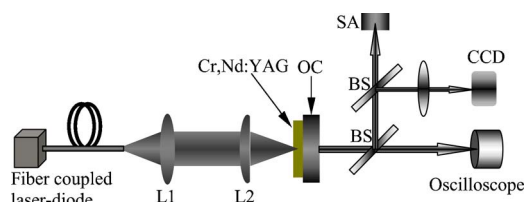*Corresponding author. E-mail address: dong@ils.uec.ac.jp

FIG. 1. (Color online) A schematic diagram of experimental setup used to generate nanosecond transverse patterns in a laser-diode pumped microchip Cr,Nd:YAG self-Q-switched laser. $L1$ and $L2$ are the focus lens; SA, spectrum analyzer; BS, beam splitter; OC, output coupler.

FIG. 2. (Color online) Average output power and repetition rate of a Cr,Nd:YAG self-Q-switched laser as a function of the Cr,Nd:YAG sample position, z, along the pump beam direction.

incident on the laser medium. The intracavity intensity will be very high for passively Q-switched solid-state laser, the inversion population will be saturated, and therefore, the saturated inversion population should be included when the transverse pattern formation was investigated. Therefore, in this paper, the effect of the pump beam and the nonlinear effect of gain medium and saturable absorber inside a Cr,Nd:YAG crystal on the transverse pattern formation of a Cr,Nd:YAG self-Q-switched microchip laser are investigated. Experimental results reveal that the transition of the transverse patterns in this microchip laser can be realized by controlling the pump beam diameter incident on the Cr,Nd:YAG crystal. The gain-guiding effect induced by the saturated inversion population and the thermal guiding effect induced by the pump power inside the gain medium play important roles on the transverse pattern formation of laser-diode pumped microchip Cr,Nd:YAG self-Q-switched laser. The observed transverse patterns were successfully reconstructed by summing different sets of Hermite-Gaussian modes under different pump conditions.

II. EXPERIMENTS AND RESULTS

Figure 1 shows the schematic diagram of a laser-diode end-pumped microchip Cr,Nd:YAG self-Q-switched laser. A plane-parallel, 1-mm-thick Cr,Nd:YAG crystal codoped with 1 at. % Nd and 0.01 at. % Cr was used as gain medium. One surface of the crystal is coated for high transmission at 808 nm and total reflection at 1064 nm. The other surface is coated for antireflection at 1064 nm and total reflection at 808 nm to increase pump power absorption. A plane-parallel output coupler with 5% transmission at 1064 nm was attached to the Cr,Nd:YAG crystal. A 3-W fiber-coupled 807 nm laser diode with a core diameter of 400 μm and numerical aperture of 0.4 was used as the pump source. Two lenses with focus length of 15 mm($L1$) and 40 mm ($L2$), respectively, were used to focus the pump beam into the crystal rear surface and to produce a pump light footprint in the crystal of about 300 μm in diameter. The laser was operated at room temperature. The Q-switched pulses were recorded by using a fast InGaAs detector of less than 1-ns rise time, and a 500-MHz Tektronix TDS 3052B-digitizing oscilloscope. The laser spectrum was analyzed by using an optical spectrum analyzer. The laser output beam profile was monitored using a charge coupled device (CCD) camera both in the near field and the far field of the output coupler.
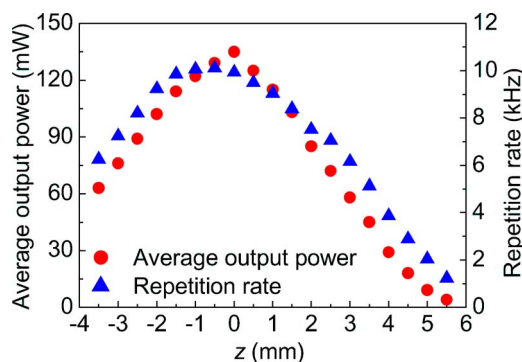
To obtain stable transverse patterns in this self-Q-switched laser, the Cr,Nd:YAG self-Q-switched laser was operated at 1.5 times above the pump power threshold when the focus point of the pump beam was just on the rear surface of the Cr,Nd:YAG crystal. By moving the Cr,Nd:YAG crystal along the pump beam direction, different sets of the transverse patterns were observed. First, average output power and repetition rate as a function of the Cr,Nd:YAG sample position (z) along the pump beam direction were shown in Fig. 2. The z=0 coordinate corresponds to a minimum measured pump beam waist of 150 μm just on the rear surface of the Cr,Nd:YAG crystal. Negative displacement of the Cr,Nd:YAG sample from z=0 indicates that the sample is close the focus lens ($L2$), positive displacement indicates the sample is far away from the focus lens ($L2$). The spot size of the pump beam increases almost symmetrically for both positive and negative displacements of the sample from z=0. Maximum average output power of 130 mW was obtained when minimum pump beam spot was just on the rear surface of the Cr,Nd:YAG crystal (z=0). Average output power decreases by moving the Cr,Nd:YAG crystal close to or away from the focus lens ($L2$) along the pump beam direction. The pump beam diameter increases when the Cr,Nd:YAG crystal is moved away from the focus point of the pump beam. The pump power intensity inside the Cr,Nd:YAG crystal decreases with increase of the pump beam diameter, therefore average output power decreases. The repetition rate had the same tendency as that for average output power with the sample position, z, however, the maximum repetition rate was obtained at z=−0.5 mm, which was not coincident with the maximum average output power at z=0. This was caused by the gain-guiding effect induced by the saturated inversion population distribution inside the Cr,Nd:YAG crystal. Pulse energy of the self-Q-switched laser was determined by average output power and pulse repetition rate. Maximum output pulse energy of approximately 13.6 μJ was obtained at z=0. Output pulse of this self-Q-switched laser was mul-tipulse oscillation or pulse with bifurcation. Figure 3(a) shows a typical output pulse profile with two pulses oscillation simultaneously at z=0. Owing to the complex transverse multimode oscillation of this Cr,Nd:YAG self-Q-switched microchip laser, output pulse trains also exhibited instabili-
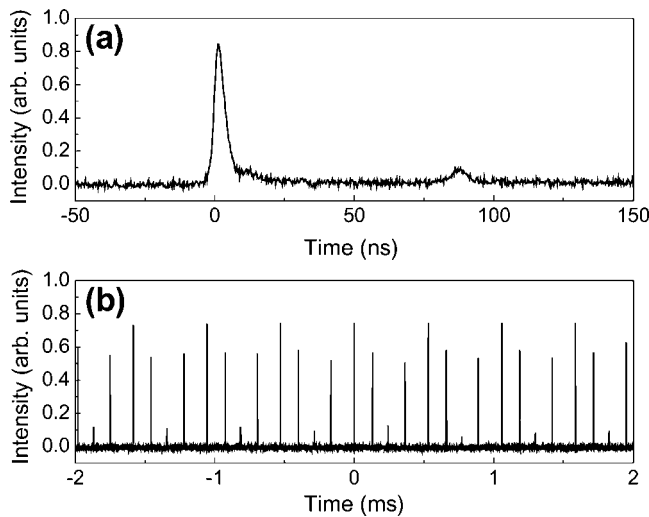
FIG. 3. (a) Typical pulse profile with two-pulse and (b) pulse train exhibited peak power instability and repetition rate jitter when the focus point of the pump beam is on the rear surface of the Cr,Nd:YAG crystal.

FIG. 4. Transverse patterns of Cr,Nd:YAG self-Q-switched laser at different Cr,Nd:YAG sample positions, z, along the pump beam direction, (a) −3.5, (b) −3, (c) −2.5, (d) −2, (e) −1.5, (f) −1, (g) −0.5, (h) 0, (i) 0.5, (j) 1, (k) 1.5, (l) 2, (m) 2.5, (n) 3, (o) 3.5, (p) 4, (q) 4.5, and (r) 5 mm.

ties and repetition rate jitters. Figure 3(b) shows a typical pulse train with periodical pulses oscillation and repetition rate jitter at $z=0$, the pulse train exhibited period-4 pulsation. Since the 1-mm-thick Cr,Nd:YAG crystal was used in the experiment, the laser was operated in the single-longitudinal-mode oscillation at such low pump power as indicated in Ref. [18]. Therefore, pulse train instability and repetition rate jitters were attributed to the multitransverse-mode competition induced by the spatial hole burning effect, the nonuniformly distribution of Cr^{4+} saturable absorber and the gain-guiding effect induced by the saturated inversion population in the Cr,Nd:YAG crystal. There should be some intrinsic relationships between output transverse patterns and corresponding pulse trains, instabilities and repetition rate jitters of pulse trains should be induced by the transverse multi-mode oscillations of a Cr,Nd:YAG microchip laser. However, since the repetition rate of the pulse train (>1 kHz) was significantly larger than the temporal resolution (30 frames per second) of the CCD camera even when the laser was operated at low repetition rate with large pump beam diameter, we did not observe any obvious relationships between the periodical pulsation and corresponding transverse patterns. It should be a very interesting topic for future experimental investigation by using high resolution CCD camera or separating the transverse modes. A pulse width [full width at half maximum (FWHM)] was in the range from 3 to 6 ns with the sample position, z. A maximum peak power of over 4.5 kW was obtained at $z=0$.

Figure 4 shows different sets of the transverse patterns observed by moving the Cr,Nd:YAG crystal along the pump direction. All observed transverse patterns have point symmetry, are very stable, reproducible, and no variation in structure over time scales of hours. The transition between two different sets of transverse patterns was found to be sudden and abruptly with slowly and gradually moving the Cr,Nd:YAG crystal along the pump beam direction. Furthermo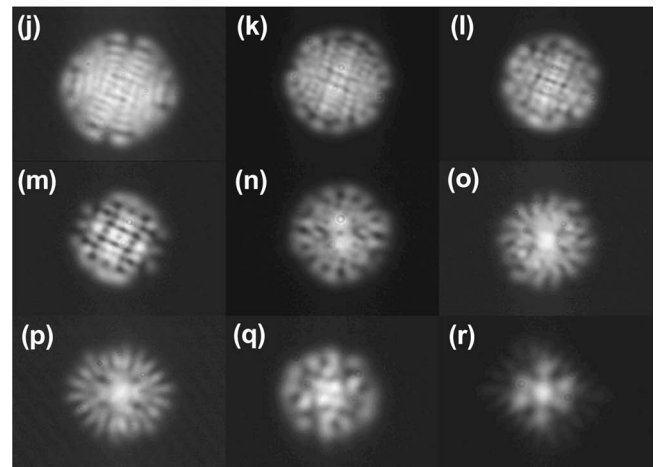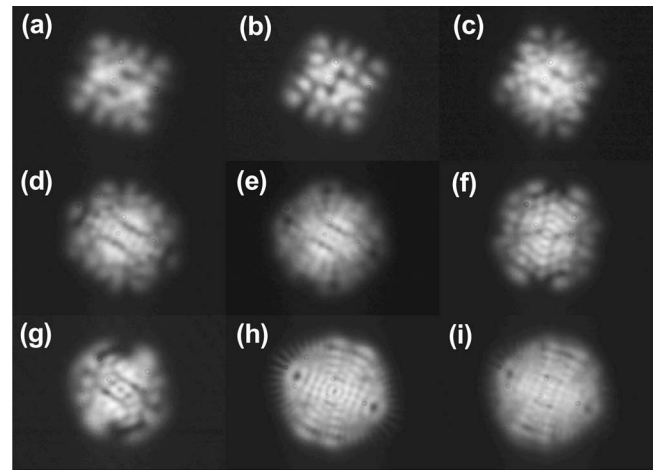re, all observed transverse patterns were preserved in free-space propagation. Although all observed transverse patterns have point symmetry and some of them are nearly circular ($z>-2$ mm), they are different from high-order Laguerre-Gaussian modes. It is well known that only Hermiet-Gaussian modes remain Hermiet-Gaussian field patterns as they propagate. Therefore, the formation of observed transverse patterns by varying the sample positions along the pump beam direction can be explained as a combination of different sets of Hermiet-Gaussian modes, we will show this combination in the next section. Figure 4(h) shows the observed transverse pattern at $z=0$. The transverse patterns are nearly circular and have point symmetry, and there are weak modes oscillating at the edge of the transverse pattern [see Fig. 4(h)]. Transverse patterns shown in Figs. 4(i) and 4(j) were kept nearly the same as that of Fig. 4(h) with further moving the Cr,Nd:YAG crystal away along the pump beam until $z=1$ mm. The weak modes at the edge of the transverse pattern disappeared at $z=1$ mm, as shown in Fig. 4(j). This was caused by the decrease of the pump power intensity

inside the Cr,Nd:YAG crystal owing to the increase of the pump beam diameter, the transverse modes at the edge of the transverse pattern were suppressed to oscillate because the gain for the transverse modes at the edge of the laser threshold. The transverse patterns were determined by the gain-guiding effect induced by the saturated inversion population distribution inside the gain medium and the nonuniformly distribution of the Cr^{4+} ions inside the Cr,Nd:YAG crystal, therefore, the spots and holes appear in the output transverse patterns. When the Cr,Nd:YAG crystal was further moved away from the focus point of the pump beam ($z > 1$ mm), the transverse patterns still kept nearly circular and had point symmetry; the numbers of the transverse-mode decreased with the increase of the pump beam diameter on the crystal [see Figs. 4(k)–4(o) and 4(r)]. The structure of the transverse patterns [Figs. 4(k)–4(o) and 4(r)] became simple compared to the transverse patterns formed near $z = 0$ [see Figs. 4(h)–4(j)]. When the sample is close to the focus lens ($z < 0$), the transverse patterns change from circular [see Figs. 4(e)–4(g)] to rectangular [shown in Figs. 4(a)–4(d)] with an increase of the pump beam diameter on the crystal, but the transverse patterns still keep point symmetry. This is a strong indication that the transverse structures of the output beam modes are really induced by the nonlinear interaction and by the spatial distribution of the pump beam, and not by the configuration of the resonator. Different structures of the output transverse patterns are due to the nonlinear saturable absorption of the Cr^{4+} ions and the gain distribution inside the Cr,Nd:YAG crystal. It is an intrinsic property of such microchip self-Q-switched lasers.

III. THEORETICAL MODELING AND ANALYSIS

The oscillation of the microchip Cr,Nd:YAG self-Q-switched laser was determined by the initial inversion population of self-Q-switched Cr,Nd:YAG laser and the inversion population distribution provided by the pump power. The initial inversion population of Cr,Nd:YAG self-Q-switched laser under continuous-wave-pumping can be expressed as [16],

$$N_i = \frac{2\sigma_g N_{s0} l + \ln\left(\frac{1}{R}\right) + \delta_{\text{Loss}}}{2\sigma l}, \quad (1)$$

where σ and σ_g are the emission cross section of gain medium and the ground-state absorption cross section of Cr^{4+} saturable absorber, N_{s0} is the total concentration of Cr^{4+} in YAG, l is the length of the Cr,Nd:YAG crystal, R is the reflectivity of the output coupler, and δ_{Loss} is the total intracavity loss. The variation of the pump power intensity on the rear surface of the gain medium with the propagation position of the pump beam can be estimated according to the expression as follows:

$$I_p(z,r) = \frac{P_{\text{in}}}{\pi w_p^2(z)} \exp\left[-\frac{2r^2}{w_p^2(z)}\right], \quad (2)$$

where z is the propagation direction of the pump beam, r is the radius of the pump beam at the z position, P_{in} is the

incident pump power on the rear surface of the gain medium and $w_p(z)$ is the beam waist at z position of the pump beam. When the pump beam incident on the gain medium is assumed to be Gaussian beam, using a beam quality factor, M^2, the radius of the pump beam along the pump direction can be expressed as [19]

$$w_p^2(z) = w_{p0}^2 \cdot \left[1 + \frac{(M^2)^2 \cdot \lambda_p^2 \cdot (z - z_0)^2}{n^2 \cdot \pi^2 \cdot w_{p0}^4}\right], \quad (3)$$

where w_{p0} is the waist of the pump beam at $z = z_0$, here z_0 is set to 0, λ_p is the pump wavelength, and n is the refractive index of the gain medium.

For a microchip laser gain medium pumped by longitudinally continuous-wave incident pump power P_{in} in a two-pass pumping configuration, the spatial distribution of the population inversion can be expressed as

$$\Delta N(r,z) = \frac{2 \cdot P_{\text{in}} \cdot \alpha \cdot f \cdot \tau}{h \cdot \nu_p \cdot \pi \cdot w_p^2(z)} \exp\left(\frac{-2 \cdot r^2}{w_p^2(z)}\right)$$
$$\times [\exp(-\alpha \cdot z) + \exp(-\alpha \cdot (2 \cdot l - z))], \quad (4)$$

where r is the radial direction in the plane transverse to the laser propagation axis, z is the direction of the laser axis, h is the Planck constant, ν_p is the frequency of the pump power, τ is the fluorescence lifetime of gain medium, α is the absorption coefficient of gain medium at pump wavelength λ_p, l is the length of the gain medium, f is the thermal population distribution fraction of the upper laser level in the crystal field component (1 for four-level system), and $w_p(z)$ is the beam waist at pump beam position z. Here, the pump beam profile has been assumed to be circular and the pump beam intensity distribution is assumed to be a Gaussian profile. Therefore, the saturated inversion population can be expressed as follows:

$$N_{\text{sat}}(r,z,\lambda) = \frac{\Delta N(r,z)}{1 + \dfrac{I_L(r,z)}{I_{\text{sat}}(\lambda)}}, \quad (5)$$

where $I_{\text{sat}}(\lambda)$ is the laser saturation intensity of the gain medium and $I_L(r,z)$ is the intensity of the laser mode inside the cavity, $I_L(r,z)$ can be expressed as [19]

$$I_L(r,z) = \frac{4P_c}{\pi w_L^2(r,z)} \exp\left[-\frac{2r^2}{w_L^2(r,z)}\right], \quad (6)$$

where P_c is the intracavity laser power, $w_L(r,z)$ is the intravaivty laser beam waist. The saturated inversion population distribution inside the 1-mm Cr,Nd:YAG crystal as a function of the thickness of the Cr,Nd:YAG crystal and pump beam radius was shown in Fig. 5. The saturated inversion population has a characteristic local minimum on axis because the laser beam waist is experimentally observed to be smaller than the pump beam radius incident on the rear surface of the Cr,Nd:YAG crystal; this has an important implication for the gain-guiding effect on the transverse modes. When the rear surface of the Cr,Nd:YAG crystal was positioned at the focus point of the pump beam, the pump area of Cr,Nd:YAG crystal was highly excited by the pump beam,
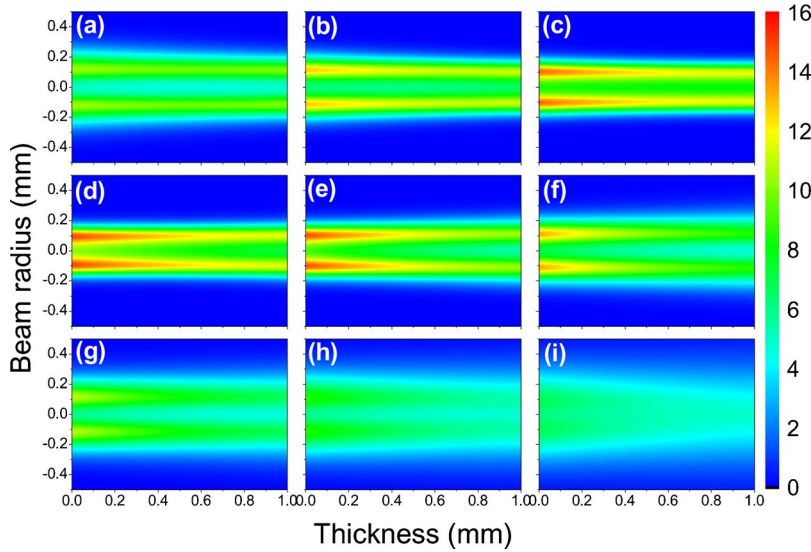
FIG. 5. (Color online) Radial variation of the saturated inversion population inside 1-mm-thick Cr, Nd: YAG crystal at different Cr, Nd: YAG sample positions, z, along the pump beam axis, (a) $z=-3$ mm; (b) $z=-2$ mm; (c) $z=-1$ mm; (d) $z=0$ mm; (e) $z=1$ mm; (f) $z=2$ mm; (g) $z=3$ mm; (h) $z=4$ mm; and (i) $z=5$ mm. The unit of inversion population is $\times 10^{24}$ cm^{-3}.

and the saturated inversion population inside the Cr, Nd: YAG crystal is higher than the initial inversion population required by the Cr, Nd: YAG self-Q-switched laser, therefore, a lot of transverse modes were excited, as shown in Fig. 4(h). Further moving the Cr, Nd: YAG crystal away from the focus point until $z=1$ mm, the transverse patterns nearly do not change [see Fig. 4(j)] because the saturated inversion population inside the Cr, Nd: YAG decreases gradually and only the saturated inversion population at the edge of the pump area was lower than the initial inversion population required by the Cr, Nd: YAG self-Q-switched laser, therefore, weak oscillating modes at the edge of the output beam vanished. Further moving the Cr, Nd: YAG sample away from the focus point, the saturated inversion population decreases further and the saturated inversion population distribution becomes flatter comparing to the tightly focused situation. So, the laser will oscillate only at those pumped areas with an inversion population higher than the initial inversion population required by the Cr, Nd: YAG self-Q-switched laser. The longitudinal saturated inversion population distribution inside the Cr, Nd: YAG microchip also had an effect on the transverse pattern formation although a 1-mm-thick Cr, Nd: YAG crystal was used in the experimental. When the Cr, Nd: YAG crystal was close to the focus lens, the transverse patterns were different from those when the Cr, Nd: YAG crystal was far away from the focus lens. This was caused by the different distribution of the saturated inversion population along the thickness of the Cr, Nd: YAG crystal when the Cr, Nd: YAG sample was placed at different position along the pump beam direction, as shown in Fig. 5. Assuming the spectral profile of the gain medium is the Lorentzian function, the gain at any positions is a function of the saturated inversion population

$$g(r,z,\lambda) = \frac{\lambda_0^2 \Delta\lambda}{16\pi^2 n^2 c\tau} \frac{N_{\text{sat}}(r,z,\lambda)}{\left(\frac{\Delta\lambda}{2}\right)^2 + \left(\frac{\lambda_0}{\lambda} - 1\right)^2}, \quad (7)$$

where n is the refractive index of gain medium at the laser wavelength, c is the speed of light in vacuum, λ is the laser wavelength, $\Delta\lambda$ is the FWHM of the gain line, and λ_0 is the central wavelength of the gain line. The change of the refractive index induced by the gain guiding effect induced by the saturated inversion population can be expressed as

$$\Delta n_{\text{gain}}(r,z,\lambda) = \frac{\lambda_0(\lambda - \lambda_0)}{2\pi\Delta\lambda} g(r,z,\lambda). \quad (8)$$

The temperature distribution induced by the pump power inside the gain medium for end-pumped microchip laser can be written as according to Ref. [20]

$$T(r,z) = T_c + \frac{P_h(z)}{4\pi k} \left\{ \ln\left(\frac{R^2}{r^2}\right) + E_i\left[\frac{2R^2}{w_p^2(z)}\right] - E_i\left[\frac{2r^2}{w_p^2(z)}\right] \right\}, \quad (9)$$

where T_c is the coolant temperature at $r=R$, r is the transverse radial coordinate, k is the thermal conductivity of the gain medium, $w_p(z)$ is the pump beam waist incident on the gain medium, R is the radius of the gain medium or the aperture of the cooler, $P_h(z)$ is the heat generated inside the gain medium when the incident pump power is P_{in}, $P_h(z) = P_{\text{in}}\alpha[\exp(-\alpha z) + R_r\exp(-2\alpha l + \alpha z)]f_h$, where α is the absorption coefficient of the gain medium at pump wavelength, l is the length of the gain medium, R_r is the reflectivity of the front surface for pump wavelength, $E_i(x)$ is the exponential integral function: $E_i(x) = \int_x^\infty \left(\frac{e^{-i}}{t}\right) dt$. Therefore, the change of refractive index due to thermal effects can be expressed as

$$\Delta n_{\text{thermal}}(r,z) = \frac{dn}{dT}\Delta T(r,z) = \frac{dn}{dT}[T(r,z) - T_c]. \quad (10)$$

The overall change of the refractive index of an active medium due to the gain-guiding effect and the thermal effect can be expressed as

$$\Delta n(r,z) = \Delta n_{\text{gain}}(r,z,\lambda) + \Delta n_{\text{thermal}}(r,z). \quad (11)$$

The field propagating in the plane-parallel microchip cavity can be described by the scalar Helmholtz wave equation as follows:
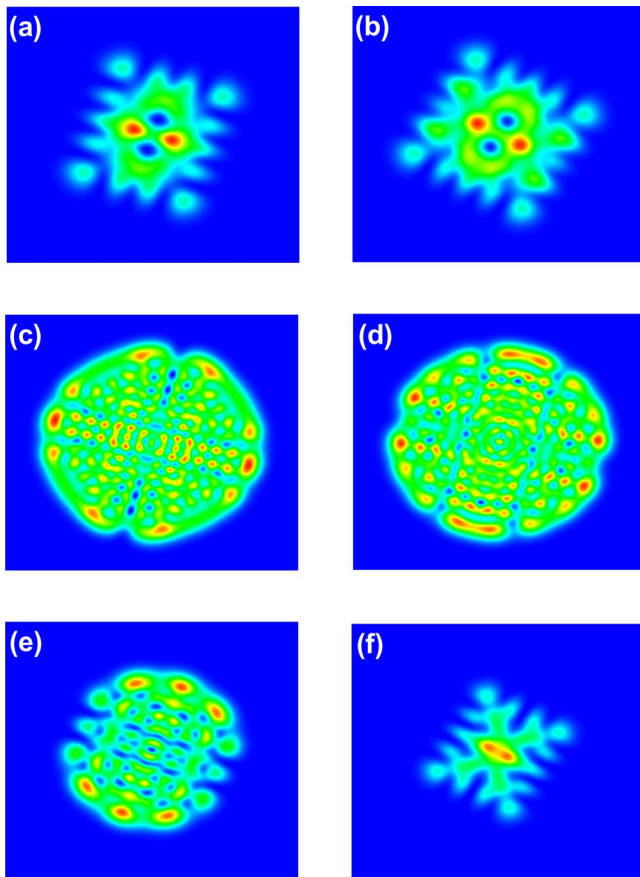
FIG. 6. (Color online) Numerical reconstruction of the observed complex transverse patterns in a laser-diode pumped Cr,Nd:YAG self-Q-switched microchip laser, (a) $z=-3$ mm; (b) $z=-2.5$ mm; (c) $z=0$ mm; (d) $z=1.5$ mm; (e) $z=2.5$ mm; and (f) $z=5$ mm.

$$(\nabla^2 + n^2 k^2)E = 0, \qquad (12)$$

where E is the complex amplitude of the electric field with time dependence of laser cavity frequency, ω, $k=\omega/c$ is the wave number in vacuum, n is the complex refractive index distribution, the imaginary part of which contains the gain and loss aspects of the medium, and c is the speed of light in vacuum. The geometry of the problem is defined entirely by the complex refractive index distribution inside the gain medium. The complex refractive index can be decomposed into two parts: the background index, n_0, is real, and the variation part, $\Delta n(r,z)$, is complex and is much smaller than the background index

$$|\Delta n(r,z)| \ll n_0, \ n(r,z) = n_0 + \Delta n(r,z). \qquad (13)$$

Therefore, the complex amplitude of the electric field can be written as follows:

$$E(r,\theta,z) = \phi(r,\theta,z)e^{ikn_0 z}, \qquad (14)$$

where r and θ are the transverse polar coordinates, z is the direction of the propagation, and $\phi(r,\theta,z)$ is the slowly varying field envelope. Substituting Eqs. (13) and (14) into Eq. (12), applying the slowly varying envelop approximation, the paraxial wave equation can be expressed as follows:

$$\left[\nabla_T^2 - 2n_0 k^2 \Delta n(r,z)\right]\phi = -2in_0 k \frac{\partial \phi}{\partial z}, \qquad (15)$$

where ∇_T^2 is the transverse Laplacian.

There were the spatial distribution variation of the saturated inversion population along the thickness of the Cr,Nd:YAG crystal when the Cr,Nd:YAG sample was placed at different positions along the pump beam. Therefore, the different transverse oscillating modes of the Cr,Nd:YAG self-Q-switched laser will be satisfied when the inversion population excited by the pump power was greater than the initial inversion population required by the Cr,Nd:YAG self-Q-switched laser, $N_{sat}(r,z,\lambda) \geq N_i$. Although the initial inversion population required by the Cr,Nd:YAG self-Q-switched microchip laser can be satisfied by the broad pump beam, the transverse mode oscillation is governed not only by the transverse distribution of the pump power inside the gain medium but also by the longitudinal distribution of the pump power inside the gain medium. Therefore, different transverse modes will be excited under different transverse distribution of the saturated inversion population along the thickness of the Cr,Nd:YAG crystal. The selection of transverse modes in the Cr,Nd:YAG microchip self-Q-switched laser is also governed by the competition of gain available for the mode oscillation and inversion population depletion by the oscillating modes. For such complex transverse mode oscillation in the Cr,Nd:YAG microchip self-Q-switched laser, transverse patterns cannot be expressed by actual solution of Eq. (14), this equation does not have an analytic solution except for a few special cases such as a quadratic index or a quadratic gain distribution [6]. Therefore, Eq. (14) must be solved numerically because the gain medium studied here includes pump power induced saturated gain profile [Eq. (7)] and thermal induced index profile [Eq. (10)] along the transverse and longitudinal direction.

However, the observed transverse patterns can be reconstructed by summing different sets of the transverse modes. The following will show the reconstruction of such complex transverse patterns observed in the experiments. Because the observed transverse patterns exhibit rectangular forms at $z<-2$ mm, therefore, the observed transverse patterns can be reconstructed by summing different sets of the Hermite-Gaussian modes. The Hermiet-Gaussian modes at different position inside gain medium can be expressed as follows:

$$HG_{m,n}(x,y) = \frac{1}{\sqrt{2^{m+n-1}\pi m!\, n!}} \frac{1}{w_L} H_m\left(\frac{\sqrt{2}x}{w_L}\right) H_n\left(\frac{\sqrt{2}y}{w_L}\right)$$
$$\times \exp\left(-\frac{x^2+y^2}{w_L^2}\right)\exp(-ikz), \qquad (16)$$

where x and y are the Cartesian coordinates, w_L is the beam waist of the laser, and H_m represents a Hermite polynomial of order m. Here some examples are given for illustrating the numerical reconstruction of the observed transverse patterns. The transverse pattern observed at $z=-3$ mm can be decomposed into $|HG_{1,0}+HG_{0,2}+HG_{3,4}|^2$, as show in Fig. 6(a). When the Cr,Nd:YAG crystal was set at $z=-2.5$ mm, the

pump power induced saturated inversion population increased, therefore, more modes can be excited, the transverse pattern observed in Fig. 4(c) can be decomposed into $|HG_{0,1}+HG_{2,0}+HG_{1,3}+HG_{4,4}|^2$, as shown in Fig. 6(b). When the Cr,Nd:YAG crystal was set to the focus spot of the pump beam, the saturated inversion population increases and will excite more oscillating modes, therefore the transverse patterns observed around focus spot can be decomposed into more complicated oscillating modes $|HG_{1,13}+HG_{2,12}+HG_{3,11}+HG_{5,9}+HG_{7,7}+HG_{9,5}+HG_{11,3}+HG_{12,2}+HG_{14,0}|^2$, as shown in Fig. 6(c). Further moving the Cr,Nd:YAG crystal away from focus point of pump beam, the inversion population decreases, the oscillating modes decrease [see Figs. 6(d) and 6(e)]. Figure 6(f) shows the reconstruction of the observed transverse pattern at $z=5$ mm by $|HG_{0,0}+HG_{1,2}+0.5HG_{4,4}|^2$. From this analysis of the pump power induced gain distribution and the thermal effect induced index distribution in Cr,Nd:YAG and the reconstruction of the transverse patterns observed in the experiments by using simple summing of the different Hermite-Gaussian modes, the transverse pattern formation in microchip Cr,Nd:YAG will be strongly governed by the distribution of the gain along the radius and longitudinal direction. Especially, the longitudinal distribution of the saturated inversion population plays a very important role in the final transverse pattern formation. Therefore, the transverse mode oscillation in the microchip laser cannot be treated as one-dimensional oscillation, the longitudinal distribution of the gain and the index distribution profile induced by the thermal effect should be taken into account.

IV. CONCLUSIONS

In conclusion, different sets of complex transverse patterns were observed in a laser-diode end-pumped Cr,Nd:YAG self-Q-switched microchip laser by using a large pump beam diameter. The observed point-symmetric transverse patterns in such a self-Q-switched laser were very stable and preserved when the laser beam propagated in the free space. Transverse pattern formation in the Cr,Nd:YAG self-Q-switched laser were mainly governed by the saturated inversion population distribution and the index distribution profile along the radius and longitudinal direction inside the Cr,Nd:YAG crystal. The gain-guiding effect was induced by the saturated gain distribution and thermal effect induced index variation along transverse and longitudinal direction inside the Cr,Nd:YAG crystal was caused by the pump power distribution inside the gain medium. The oscillation modes in the Cr,Nd:YAG microchip laser were governed by the initial inversion population required by the Cr,Nd:YAG laser and the gain distribution along the thickness of the Cr,Nd:YAG crystal. The pump beam diameter has a great influence on the pattern structure, average output power, pulse repetition rate, and pulse profiles. The observed transverse patterns were successfully reconstructed by summing different sets of Hermiet-Gaussian modes. The output beam with different transverse patterns and several kilowatt (kW) peak power will be a good candidate to generate light fields with a nontrivial transverse distribution of quantum fluctuations and which can be useful to increase the transverse resolution in optical image processing.

[1] Q. Feng, J. V. Moloney, and A. C. Newell, Phys. Rev. A **50**, R3601 (1994).

[2] D. Dangoisse, D. Hennequin, C. Lepers, E. Louvergneaux, and P. Glorieux, Phys. Rev. A **46**, 5955 (1992).

[3] E. Louvergneaux, D. Hennequin, D. Dangoisse, and P. Glorieux, Phys. Rev. A **53**, 4435 (1996).

[4] G. Huyet, M. C. Martinoni, J. R. Tredicce, and S. Rica, Phys. Rev. Lett. **75**, 4027 (1995).

[5] S. P. Hegarty, G. Huyet, P. Porta, J. G. Mclnerney, K. D. Choquette, K. M. Geib, and H. Q. Hou, J. Opt. Soc. Am. B **16**, 2060 (1999).

[6] W. Nakwaski and R. P. Sarzala, Opt. Commun. **148**, 63 (1998).

[7] K. Otsuka, P. Mandel, and E. A. Viktorov, Phys. Rev. A **56**, 3226 (1997).

[8] G. Martel, C. Labbe, F. Sanchez, M. Fromager, and K. Kit-Ameur, Opt. Commun. **201**, 117 (2002).

[9] C. Serrat, M. P. v. Exter, N. J. v. Druten, and J. P. Woerdman, IEEE J. Quantum Electron. **35**, 1314 (1999).

[10] S. Longhi, G. Cerullo, S. Taccheo, V. Magni, and P. Laporta, Appl. Phys. Lett. **65**, 3042 (1994).

[11] G. K. Harkness and W. J. Firth, J. Mod. Opt. **39**, 2023 (1992).

[12] S. Longhi, J. Opt. Soc. Am. B **11**, 1098 (1994).

[13] J. J. Zayhowski, J. Alloys Compd. **303-304**, 393 (2000).

[14] A. A. Ishaaya, N. Davidson, and A. A. Friesem, Opt. Express **13**, 4952 (2005).

[15] M. Wei, C. Chen, and K. Tu, Opt. Express **12**, 3972 (2004).

[16] J. Dong, J. Lu, and K. Ueda, J. Opt. Soc. Am. B **21**, 2130 (2004).

[17] P. Wang, S. Zhou, K. K. Lee, and Y. C. Chen, Opt. Commun. **114**, 439 (1995).

[18] J. Dong and K. Ueda, Appl. Phys. Lett. **87**, 151102 (2005).

[19] T. Taira, J. Saikawa, T. Kobayashi, and R. L. Byer, IEEE J. Sel. Top. Quantum Electron. **3**, 100 (1997).

[20] M. E. Innocenzi, H. T. Yura, C. L. Fincher, and R. A. Fields, Appl. Phys. Lett. **56**, 1831 (1990).